ELSEVIER

Biochimica et Biophysica Acta 1524 (2000) 110–117

BIOCHIMICA ET BIOPHYSICA ACTA
BBA

www.elsevier.com/locate/bba

Gel–sol transition can describe the proteolysis of extracellular matrix gels

Hugues Berry [a], Juan Pelta [a], Didier Lairez [b], Véronique Larreta-Garde [a,*]

[a] *ERRMECE, University of Cergy-Pontoise, 2 av. A. Chauvin, B.P. 222, 95302 Cergy-Pontoise Cedex, France*
[b] *Laboratoire Léon Brillouin, CEA-CNRS, CEA/Saclay, Saclay, France*

Received 29 June 2000; received in revised form 18 September 2000; accepted 21 September 2000

Abstract

We monitored the cell-free solubilization of extracellular matrix and fibronectin gels, catalyzed by exogenous proteinases. The corresponding measurements could not be interpreted according to usual proteinase kinetics. The observation that this experimental system did not consist in surface but in bulk degradation and appeared specific to gel substrates, incited us to use gelation-related approaches to describe these kinetics. We show that the gel–sol transition theory adequately describes the enzyme reactions. This allowed formulation and experimental confirmation of a power law relating macroscopic changes of the gel to enzyme kinetics. This approach could also be used for other power laws predicted by the gel–sol transition theory, allowing a better understanding of macroscopic modification of the extracellular matrix during proteolysis, which is implied in many biological situations, especially tumor dissemination.

Keywords: Extracellular matrix; Proteinase; Gel; Sol–gel transition

1. Introduction

The extracellular matrix (ECM) is a dense network of various proteins including collagens, elastin, fibronectin and laminin, among others [1]. In mammals, the ECM forms basement membranes and the underlying interstitial stroma. These dense matrices are insoluble barriers that are normally impermeable to cell passage. Thus the ECM ensures organ integrity by insulating the organs and preventing cell dissemination to remote locations. Moreover, the ECM is the support of cell adhesion and thus regulates cell proliferation, differentiation and locomotion [2,3]. During specific processes, especially tumor dissemination (metastasis), some cells acquire the ability to traverse the ECM [4]. This capacity to invade the connective tissue allows them to access the lymphatic and blood circulation and thereby to disseminate into distant organs.

To penetrate the connective tissue, invasive cells must modify the environment of the ECM in order to increase its permeability. To this end, they are believed to produce proteinases in the ECM [5,6], or to induce proteinase secretion from surrounding host cells [7,8]. In agreement with this hypothesis, numerous ECM-degrading proteinases, especially metalloproteinases (MMP), have been correlated with tumor invasiveness or metastatic potential [9,10]. Moreover, knock-out experiments on proteinase genes [11] or administration of specific inhibitors [12,13] have further established the involvement of these enzymes in tumor dissemination.

Nevertheless, the mechanisms whereby proteinase activity permits tumor invasion through the matrix are still unclear. Actually, the difficulty arises from the fact that cell invasion implies macroscopic changes in the ECM, whereas proteinase activity can be described only in terms of a molecular reaction (peptide bond hydrolysis). Thus, describing the relations between the proteinase reaction and the resultant ECM macromolecular modifications would contribute further insight into the mechanisms of tumor invasion.

In this paper, we studied the degradation in vitro of ECM gels by exogenous proteinases, i.e., under cell-free conditions. The kinetics of gel solubilization were monitored with a spectrophotometric assay that measures the appearance of solubilized hydrolysis products during the

* Corresponding author. Fax: +33-1-3425-6552;
E-mail: larreta@u-cergy.fr

0304-4165/00/$ – see front matter
PII: S0304-4165(00)00144-6

reaction. We showed that the unusual kinetics observed can be interpreted in terms of a gel–sol transition.

2. Materials and methods

2.1. ECM gel preparation

'ECM gel' from Sigma is a cell- and fibronectin-free basement membrane extracted from mouse sarcoma, with a total protein concentration of approximately 12 g l^{-1}. This preparation is liquid at temperatures below 15°C and reversibly gels at higher temperatures. A sample of 50 μl of 'ECM gel' preparation was transferred at 4°C to a 1.6-ml quartz cuvette and gelation was obtained by incubation for 1 h at 37°C. This gel is formed by weak, non-covalent interactions, as attested by gelation reversibility with temperature.

2.2. Fibronectin gelation

Fibronectin is a large protein (5.5 10^5 g mol^{-1}) found in plasma and many extracellular matrices where it mediates cell adhesion to the ECM. It has been purified to 98.6 ± 1.2% homogeneity (w/w) from cryoprecipitated human plasma [14]. Fibronectin in 25 mM Tris–HCl buffer (pH 7.4) containing 0.5 mM EDTA was concentrated to 11.0 g l^{-1} (the molar extinction coefficient is 704×10^3 mol^{-1} 1 cm^{-1} [15]) using Ultrafree-15 centrifugal concentrators from Millipore. Covalent fibronectin gels were formed directly in a 1.6-ml quartz cuvette by addition of 8.0 μl glutaraldehyde (Merck, 1.25% (v/v) in water) to 42.0 μl of the concentrated fibronectin solution. After 16 h of polymerization at 4°C, 50 μl of a water-insoluble chemical gel was obtained at the bottom of the cuvette. To remove excess glutaraldehyde, the gel was rinsed three times at room temperature with 50 mM Tris–HCl buffer (pH 7.4) containing 5 mM $CaCl_2$.

2.3. Enzymes

Thermolysin (EC 3.4.24.27, protease type X from *Bacillus thermoproteolyticus rokko*, Sigma) is a zinc metalloproteinase. Trypsin (EC 3.4.21.4, from bovine pancreas, Boehringer Mannheim) and proteinase K (EC 3.4.21.14, from bovine pancreas, Boehringer Mannheim) are serine proteinases. All enzymes were stored at −75°C as 1 g l^{-1} stock solutions in 50 mM Tris–HCl buffer (pH 7.4) and diluted extemporaneously to the desired concentration in the same buffer. For ECM gel degradation, 5 mM EDTA was also added to the dilution buffer to avoid endogenous metalloproteinase activity in the gel.

2.4. Enzyme reference activity

To compare the catalytic efficiency of the three proteinases, a reference activity (A_r) was determined on a classical soluble substrate [16]. Enzymes were added to a 0.6% azocasein (Sigma) solution, in 100 mM Tris–HCl buffer (pH 7) at 37°C. At regular intervals, a 500-μl aliquot of the reaction mixture was stopped by addition of 100 μl trichloroacetic acid (50% (w/v) in water), then centrifuged for 10 min at $8000 \times g$. Next, 550 μl of the supernatant was neutralized with 365 μl of 2 M NaOH. The extent of the reaction was determined by measurement of absorbance at 440 nm, due to azo groups of trichloroacetic acid-solubilized peptides. The reference activity (A_r) of each enzyme under these conditions was expressed as a ratio of the catalytic constant k_{cat} for the enzyme considered to that of thermolysin: $A_r^{trypsin} = 0.083$, $A_r^{proteinase\ K} = 0.400$, and $A_r^{thermolysin} = 1$.

2.5. Enzyme-catalyzed degradation of the gels

ECM or fibronectin gels were used immediately after preparation. The proteolysis reaction was initiated by addition of 1.0 ml of the enzyme solution to 50 μl of gel, and heated to 37°C. Under these conditions, the gels do not spontaneously solubilize in the absence of enzyme.

Initially, then, the experimental system comprises two distinct areas (see Fig. 1). In the bottom of the cuvette is the area formed by the gel itself, referred to as the 'matrix' area. Above it, is the area that initially consists of the proteinase solution, referred to as the 'liquid' area. As the reaction begins, some enzyme molecules diffuse from the liquid to the matrix area, catalyzing the formation of hydrolysis products in the matrix. At this point, the matrix area itself consists of two phases: an insoluble phase formed by the gel network, referred to as the 'gel' phase of the matrix area, and a soluble phase formed by the enzyme and the solubilized proteolysis products, referred to as the 'sol' phase of the matrix area.

As the reaction proceeds, the solubilized products diffuse from the sol phase of the matrix area, to the liquid area. The solubilization kinetics are monitored by measuring the appearance of these products in the liquid area (light absorbance of the liquid area at 280 nm). This signal reveals the total concentration of amino acids that diffuse out of the matrix area to the liquid area, independently of the size or mass of the polypeptides they form. For this reason, the proteolysis reaction that occurs in the liquid area is not monitored: the magnitude of the $A_{280\,nm}$ signal is thus a measure of the enzyme-catalyzed solubilization of the matrix area. The $A_{280\,nm}$ measurements were performed without stirring, and it has been verified that hand-stirring of the liquid area during the reaction does not qualitatively change the kinetics (data not shown).

2.6. Estimation of gel parameters and variables

The raw signal measured, $A_{280}(t)$, was used to estimate the sol fraction of the matrix area, at the respective reac-

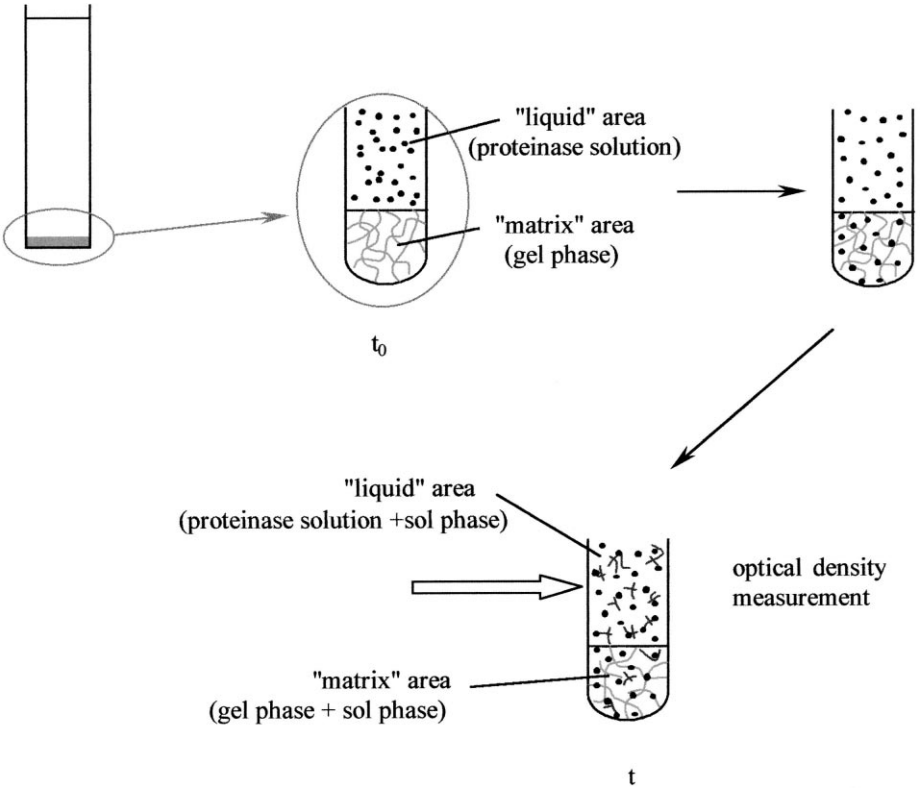

Fig. 1. Schematic representation of the experimental system for ECM and fibronectin gel proteolysis. The matrix area volume is 20 times less than that of the liquid area (upper, left). The organization of the different phases is shown as magnified views of the total system, for three reaction points: reaction initiation by the enzyme in the liquid area (t_0, upper left) is induced by enzyme penetration into the matrix area (upper right). In the matrix area, the proteolysis reaction solubilizes proteins from the gel phase to the sol phase of the matrix. These solubilized products then diffuse from the matrix to the liquid area, where optical density measurement monitors their appearance (t, bottom). See Section 2 for further details.

tion time (see Section 3) using: $X_{sol}(t) = A_{280}(t)/A_0$, were A_0 is the 280 nm absorbance of the matrix area before gelation, corrected by the adequate dilution factors (i.e., glutaraldehyde volume for fibronectin gels, and that of the liquid area for both gels). X_{gel} is obtained at each reaction times using: $X_{gel}(t) = 1 - X_{sol}(t)$. As A_{280} is found to be a linearly increasing function of time, $X_{gel}(t)$ is linearly decreasing. A linear regression on the curve $X_{gel} = f(t)$ yields the total solubilization time t_c (extrapolation to $X_{gel} = 0$). This value is then used to plot X_{gel} as a function of ε, in log–log coordinates. β is determined as the slope of this last graphic representation. The β value presented are averages and standard deviations on all the tested concentrations of the enzyme under consideration (each experiment being realized in triplicate).

3. Results

3.1. ECM gel degradation

Fig. 2 shows the degradation kinetics of ECM gels by three different trypsin concentrations. A similar profile was observed regardless of enzyme concentration: after an initial common 'bump', product concentration in the liquid phase increased linearly to a threshold value where it abruptly became constant. As control experiment, incubation of ECM gel for 72 h under the same conditions, but with zero enzyme concentration yields a constant $A_{280\,nm}$, corresponding to that of the buffer (data not shown). $A_{280\,nm}$ variations are thus enzymatically induced.

Whatever the enzyme concentration, the absorbance at the threshold was constant within experimental error, and corresponded to the quantity of protein initially included in the matrix area. This indicates that all the proteins were transformed into soluble products. It should be kept in mind that all throughout the reaction, proteolysis occurs in the liquid area but, inasmuch as this does not modify the global quantity of amino acids in this area, the measured signal only reveals the solubilization of the gel phase (see Section 2).

The kinetics observed here differed considerably from the usual kinetic profile of proteinases, which is normally characterized by a long post-stationary phase due to the progressive appearance of new cleavable bonds revealed by hydrolysis and to the expression of proteinase selectivity [17]. In Fig. 2, the evolution of hydrolysis products displays a 'bump' followed by a linear phase, and the

usual monotonic decrease in the reaction rate that signals the post-stationary phase, is absent. In all enzymatic reactions, the absence of a post-stationary phase is only obtained when a large enzyme to substrate concentration ratio is used. In this case, equilibrium is very rapidly attained after a short quasi-linear phase [17]. Here, this particular condition was not fulfilled. The fact that the ECM gel is a particularly complex system composed of many different proteins and glycoproteins might account for the complex kinetics observed here. To better understand the solubilization kinetics, we studied the degradation of simpler experimental models of ECM.

3.2. Fibronectin gel degradation

Fibronectin is an ECM glycoprotein that plays a key role in ECM assembly [18,19], cell adhesion [20,21] and tumor dissemination [22]. In vivo, its inclusion into ECM involves both weak interactions and covalent binding [23]. We studied fibronectin gels obtained by glutaraldehyde covalent crosslinking. The degradation kinetics of these gels are presented in Fig. 3 for three different thermolysin concentrations. The same profiles were obtained with trypsin or proteinase K. These kinetics were comparable to those observed with ECM gels, except for the initial 'bump' which was not present with fibronectin gels. Incubation of fibronectin gels for 72 h under the same conditions, but with zero enzyme concentration yields a constant $A_{280\,nm}$ corresponding to that of the buffer (data not shown), indicating that $A_{280\,nm}$ variations are enzymatically induced.

The interpretation of the kinetics strongly depends on the balance between enzyme activity and enzyme diffusion from the liquid to the matrix area (see Fig. 1). During fibrin clot degradation by various proteinases, enzyme diffusion in the clot is much slower than the reaction, leading to surface degradation of the clot during which clot height decreases under the action of the enzyme [24]. In the case

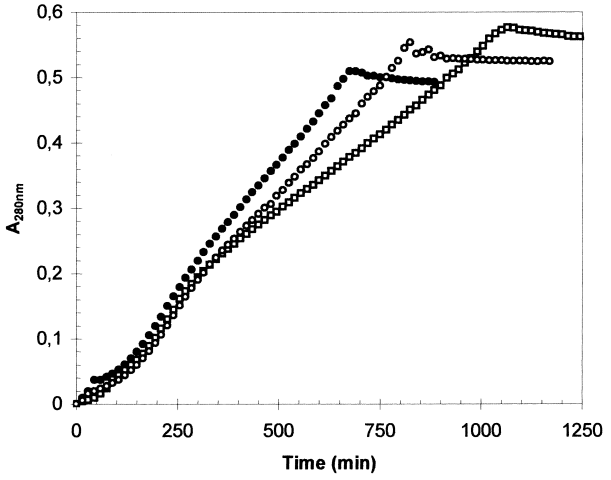

Fig. 2. Typical degradation kinetics of ECM gels. Solubilization catalyzed by 0.70 (□), 1.50 (○), and 5.50 (●) μM trypsin, at 37°C.

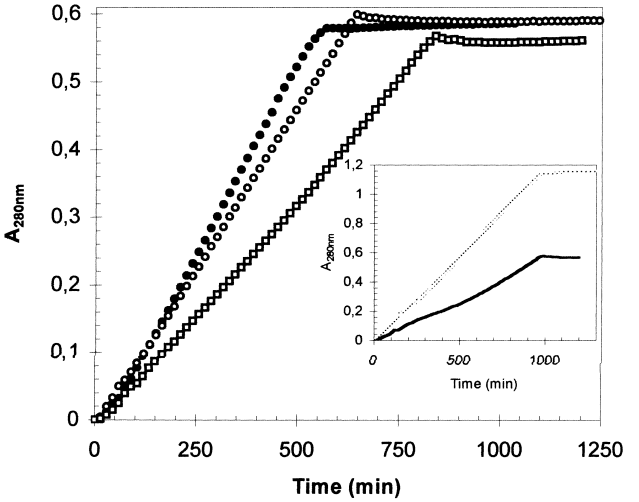

Fig. 3. Typical degradation kinetics of cross-linked fibronectin gels. Solubilization catalyzed by 0.113 (□), 0.560 (○) and 0.968 (●) μM thermolysin, at 37°C. Inset: solubilization of 50 μl (solid line) and 100 μl (diffuse line) fibronectin gels by 0.325 μM thermolysin at 37°C. In both experiments, the surface contact between the matrix and the liquid areas is constant.

of the gels studied here, a simple visual inspection revealed no evidence for such a mechanism. Furthermore, under surface degradation conditions, the time required for the total solubilization of the matrix area should be dependent on the initial height of this area. The inset in Fig. 3 shows that doubling the height of the matrix area (but preserving the same contact surface with the liquid area) did not modify the solubilization time. This result validates the alternative hypothesis of a homogenous distribution of the enzyme in the matrix area before the reaction has proceeded to a notable extent: the hydrolysis proceeds through volume degradation rather than surface degradation of the matrix area.

3.3. Interpretation of the solubilization kinetics

The common features of both ECM and fibronectin gel degradation (linear kinetics as the reaction approaches the solubilization point, sharp slope change at this point) were found to be specific to gel degradation, since they were not observed during the degradation of soluble or insoluble aggregated fibronectin (data not shown). Thus, we were particularly interested in the evolution of parameters describing the gel state of the insoluble substrate during proteolysis.

Considering the high substrate to enzyme concentration ratio in the matrix area, a quasi-steady-state approximation (QSSA, [25]) for the reaction can be assumed. This means that the substrate consumption rate in this area is constant. The actual substrates of a proteolytic reaction are the peptide bonds, which are also the elementary links that form the insoluble network of the matrix phase. Defining p as the number of such links in this network, the quasi-stationary state assumption means: dp/dt = constant,

or, equivalently:

$$p \propto t \quad (1)$$

This allows the kinetics to be related to the connectivity in the matrix area. As the observed kinetics appeared specific to gels, we attempted to describe the reaction using variables that are classically employed in gelation theory: the sol–gel transition theory [26]. This theory predicts laws for the evolution of the characteristics of a liquid medium undergoing gelation. As gelation proceeds, soluble chains randomly bind to form growing soluble clusters which assemble to form a gel. The passage from a liquid to a gelled insoluble state, namely the sol–gel transition, is a critical phenomenon [27]. At the critical gelation threshold, a slight variation in the bond quantity induces the formation of a cluster whose size is on the order of the recipient size (infinite cluster) [28]. This very point represents the transition from the soluble to the gelled state. Near this critical gelation threshold, the sol–gel transition theory predicts that the variables describing the gel (distance to the threshold, sol or gel fraction, mesh size, etc.) are inter-related by power law relationships, whose corresponding exponents are referred to as critical exponents. Actually, this theory usually describes the transition from the soluble to the gel state, but the reverse transition (from the gel to the soluble phase) also comes under the same theoretical framework.

Using Eq. 1, the relative distance to the threshold $\varepsilon = |p\text{-}p_c|/p_c$ (where p_c stands for the value of p at the gelation threshold) can be expressed as:

$$\varepsilon = 1 - t/t_c \quad (2)$$

where t_c is the time corresponding to the total solubilization of the matrix area. The sol fraction, X_{sol}, is the fraction of protein in the matrix area that belongs to the sol phase. Here, for each time (see also Section 2):

$$X_{sol} = A_{280}/A_0 \quad (3)$$

where A_0 is the initial quantity of protein in the matrix area (estimated from its A_{280} before gelation). The gel fraction (fraction of protein in the matrix area that belongs to the gel phase) is $X_{gel} = 1 - X_{sol}$. For both ECM and fibronectin gels, and close to the solubilization threshold, A_{280} is found to be a linear function of time. Combining (Eqs. 2 and 3), one thus expects:

$$X_{gel} \propto \varepsilon \quad (4)$$

This can be further verified in Fig. 4, where data from

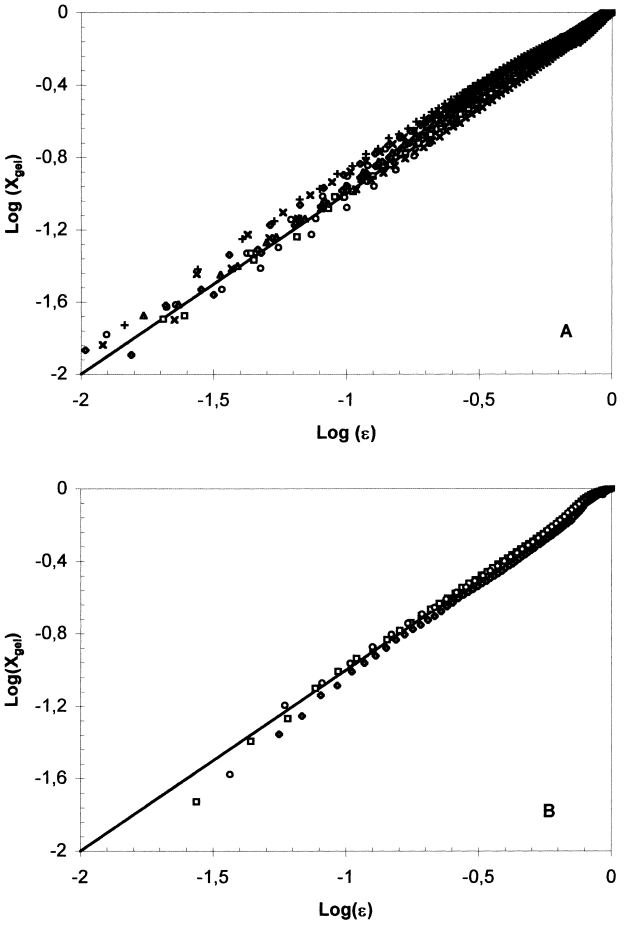

Fig. 4. X_{gel} dependence on ε for (A) thermolysin-degraded fibronectin gels and (B) trypsin-degraded ECM gels. (A) Fibronectin gel degradation catalyzed by 0.968 (○), 0.560 (□), 0.325 (◇), 0.202 (△), 0.056 (×) or 0.027 (+) μM thermolysin. (B) ECM gel degradation catalyzed by 5.50 (○), 1.50 (□) or 0.70 (◇) μM trypsin. These data are obtained by recasting the results of experiments similar to those presented in Figs. 2 and 3, in order to obtain X_{gel} and ε for each time interval. The solid lines represent $X_{gel} = \varepsilon^1$, and are given as visual guides.

experiments similar to those shown in Figs. 2 and 3 are recast to express X_{gel} as a function of ε in log–log coordinates. This figure shows that for both types of gels and regardless of enzyme concentration, X_{gel} is proportional to ε (Eq. 4). This proportionality can be compared to the power law (predicted by gelation theory):

$$X_{gel} \propto \varepsilon^{\beta} \quad (5)$$

where β is one of the critical exponents. In the case of the gels studied here, this law is observed both for gels and for the three proteinases used, with $\beta = 1$ (Table 1). Note that

Table 1
Measured values of the exponent β ($X_{gel} \propto \varepsilon^{\beta}$) for fibronectin or ECM gel degradation by thermolysin, trypsin and proteinase K

Fibronectin gels			ECM gels
Thermolysin	Trypsin	Proteinase K	Trypsin
1.05 (±0.10)	1.02 (±0.04)	1.06 (±0.05)	1.01 (±0.03)

For each initial enzyme concentration, experiments are realized in triplicate. Presented are the β values averaged over all the tested initial concentrations of the enzyme under consideration, as well as the corresponding standard deviation (in parentheses).

this β value is precisely the value predicted by the mean-field theory of sol–gel transitions [29].

These results therefore show that the degradation of ECM and fibronectin gels can be described by the sol–gel transition theory. This theory predicts that the mechanisms governing the evolution of some of the variables describing the gel, such as the gel fraction, are quite general, so that the power laws describing the behavior of these variables do not depend on details of the particular experimental system [30]. In agreement with this principle, the β value determined in the present work does not depend on the specificity or the activity of the enzyme. It is also independent of the nature of the links allowing gel formation: covalent links for fibronectin gels, or weak reversible links for ECM gels (Table 1).

3.4. Dependence of solubilization time on proteinase concentration

The reaction time required for total solubilization of the matrix area (t_c) varied experimentally with enzyme initial concentration. More precisely, $1/t_c$ was found to vary linearly with the enzyme concentration, for both ECM and fibronectin gels, and for the three enzymes used. As presented in Fig. 5 (inset), the corresponding slopes were dependent of the enzyme used.

Nevertheless, when plotted against the enzyme concentration multiplied by the reference activity of the concerned enzyme (see Section 2), the t_c^{-1} values for the three enzymes and for both gels were found to be aligned on a single straight line, with equation (Fig. 5):

$$t_c^{-1} = b \times A_r \times [E] + c \quad (6)$$

where [E] is the enzyme concentration, A_r its reference activity, and b and c are the parameters from the linear regression in Fig. 5 (the slope $b = 8.08 \times 10^{-4}$ $\mu M^{-1}\,min^{-1}$ and the interpolated t_c^{-1} value at zero enzyme concentration, $c = 8.70 \times 10^{-4}$ min^{-1}).

Eq. 6 is independent of the specificity of the enzymes and independent of the gels studied in this work. This means that the diversity of the peptide bonds encountered by the proteinases in both the ECM and fibronectin gels is large enough for the proteolysis rate to not be limited by enzyme specificity.

Further, it defines a direct relation between the solubilization threshold and the enzyme concentration and activity. It can be used to eliminate t_c from Eq. 2. This predicts the time evolution of the gel or sol phases in the matrix area, as a function of time and enzyme concentration:

$$X_{gel} \propto 1 - t \times (b \times A_r \times [E] + c) \quad (7)$$

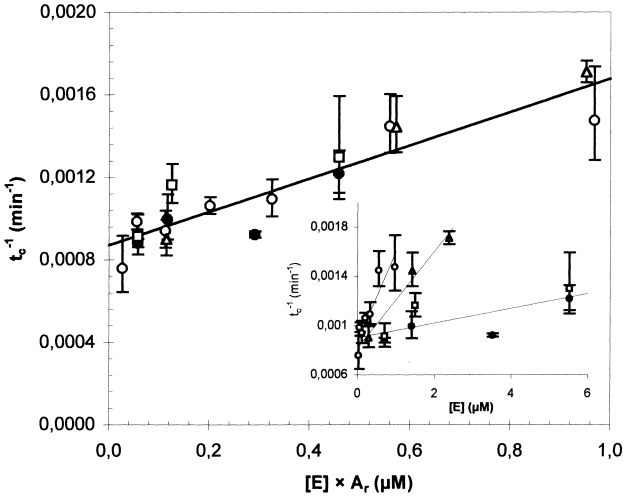

Fig. 5. t_c^{-1} dependence on enzyme concentration. t_c^{-1} values are plotted against the enzyme concentration ([E]) multiplied by the relative activity of the enzyme under consideration (A_r, see Section 2) for fibronectin gel degradation by thermolysin (○), trypsin (●) or proteinase K (△) and for ECM gel degradation by trypsin (□). Inset: the same t_c^{-1} values as in the main panel are plotted against enzyme concentration ([E]) only. The symbols for the enzymes are the same as above. The solid lines represent linear regressions.

4. Discussion

4.1. Physiological applications

In this work, the proteolysis of ECM and fibronectin gels was studied by monitoring solubilization, rather than protein degradation. So far, no kinetic model has been available to describe such an enzyme-catalyzed reaction. The kinetic profiles we observed were specific for gel degradation, and the experimental conditions were such that the solubilization did not proceed by surface degradation. We showed that, in this case, the solubilization kinetics can be described by the sol–gel transition theory, which furnishes an appropriate formalism for gelled substrate solubilization. In agreement with the properties of sol–gel transitions, we observed that the resulting law was not dependent on enzyme specificity or on gel type. This indicates that the sol–gel transition theory can adequately describe ECM solubilization kinetics in vivo if enzyme diffusion in the ECM is high enough to avoid surface degradation.

An interesting feature of the sol–gel transition theory is the ability to predict power laws for the macroscopic characteristics of the gel [26]. One such law expresses X_{gel} as a function of ε (Eq. 5), and has been experimentally observed in this paper. Other power laws express macroscopic quantity as a function of ε or of each other. For example, the correlation length ξ of the network (the characteristic size of the mesh) scales as: $\xi \propto \varepsilon^{-\nu}$. The viscosity η (for $p < p_c$) and the elastic modulus G (for $p > p_c$) behave as: $\eta \propto \varepsilon^{-s}$, and $G \propto \varepsilon^{t}$, respectively [29]. These laws reveal critical exponents (ν, s and t), whose values are

predicted by the sol–gel transition theory. In fact, these macroscopic characteristics are precisely the pertinent parameters to describe cell invasion through the ECM. Indeed, the primary goal of extracellular proteinase activity in the case of tumor invasion is to increase the ECM mesh size which, in turn, increases ECM permeability towards the cell. Moreover, ECM proteolysis modifies not only the biochemistry of the cell environment, but also its purely mechanical characteristics (ECM porosity, stiffness, rigidity). These mechanical properties in turn crucially influence cell adhesion, protein (including proteinases) expression, or locomotion [31–33]. The understanding of the influence of proteolysis on cell invasion thus partly implies the understanding of its influence on ECM mechanical characteristics. Using the same approach as that used in the present paper, these mechanical characteristics could be related to enzyme kinetics through the power laws predicted by the sol–gel transition theory.

4.2. Critical transition

The experiments reported here lead to a critical exponent value $\beta = 1$. Two theoretical models attempt to describe gelation: the mean field theory, which precisely predicts $\beta = 1$, and percolation in three dimensions, which predicts $\beta = 0.44$ [29]. Thus our results are consistent with the mean-field model, although most of the experimental studies of gelation agree with percolation rather than mean-field theory [26]. However, note that the mean-field theory has recently been shown to describe the kinetics of bulk degradation (as opposed to surface degradation) of cross-linked artificial hydrogels by non-enzymatic hydrolysis [34,35]. Several explanations can be invoked to account for the critical behavior observed here, and are listed below by way of hypothesis:

1. The main difference between the percolation and mean-field models lies in excluded volume interactions, which are neglected in the latter. Excluded volume interaction means that the elementary units connected together are unable to interpenetrate each other. Theoretically, in fact, this is always the case at the critical gelation threshold. However, at finite distances from the threshold, excluded volume interactions can be neglected in the particular case of gelation occurring between interpenetrated polymer coils [36]. It is noteworthy that the formation of fibronectin gels is accompanied by syneresis (a small portion of solvent is expelled from the gel) and thermodynamic microphase separation (the gel is turbid). This is a consequence of an overlap and a partial collapse of fibronectin aggregates formed before the gelation itself. As far as ECM gels are concerned, collagen, their main constituent, is presumably in a semi-dilute state at the concentrations studied here, i.e., collagen chains are already interpenetrated. Thus, both fibronectin chemical gels and ECM gels can fulfil the condition for the observed mean-field exponent. However, further investigations are needed to understand the role of syneresis and microphase separation in the observed critical behavior.
2. The manner in which the sol fraction was measured assumes free diffusion of the solubilized molecules from the sol phase of the matrix area to the liquid area. This may not be the case for some very large clusters in the sol phase, where steric hinderance may prevent their diffusion to the liquid area. In such a case, the measured population would not reflect the entire solubilized protein population.
3. In the percolation model, not every link that is created (or broken for reverse gelation and gel degradation) is efficient with respect to the increase (or decrease) of the gel fraction. Small loops within the gel can occur, but the link may also concern two soluble clusters. This is the reason why the β exponent value for percolation is lower than that predicted by the mean field theory, which neglects this feature. In the case of the experiment reported here, the gel phase is covered by the liquid area which is assumed to empty the gel of its sol phase. The remaining enzyme substrate in the 'matrix' area is therefore mainly the gel itself (rather than gel plus sol phase as for the percolation model). This might lead to a more efficient catalysis with respect to gel degradation.

To clarify this point, further characterizations of the sol population would be of interest and could be performed by light scattering and small-angle neutron scattering. Although difficult to adapt to the kind of gels studied in this work, these techniques would allow measurement of the soluble cluster weight-averaged molecular mass and radius of gyration, both before and after the gel point and during proteolysis.

References

[1] J.T. Price, M.T. Bonovich, E.C. Kohn, Crit. Rev. Biochem. Mol. 32 (1997) 175–253.
[2] R.K. Assoian, J. Cell Biol. 136 (1997) 1–4.
[3] J. Heino, Int. J. Cancer 65 (1996) 717–722.
[4] L.A. Liotta, P.S. Steeg, W.G. Stetler-Stevenson, Cell 64 (1991) 327–336.
[5] Z. Werb, Cell 91 (1997) 439–442.
[6] G. Murphy, J. Gavrilovic, Curr. Opin. Cell Biol. 11 (1999) 614–621.
[7] H. Guo, S. Zucker, M.K. Gordon, B.P. Toole, C. Biswas, J. Biol. Chem. 272 (1997) 24–27.
[8] D.L. Orstein, J. MacNab, K.H. Cohn, Clin. Exp. Metastasis 17 (1999) 205–212.
[9] H. Nakahara, L. Howard, E.W. Thompson, H. Sato, M. Seiki, Y. Yeh, W.T. Chen, Proc. Natl. Acad. Sci. USA 94 (1997) 7959–7964.
[10] M.I. Cockett, G. Murphy, M.L. Birch, J.P. O'Connel, T. Crabbe, A.T. Millican, I.R. Hart, A.J.P. Docherty, Biochem. Soc. Symp. 63 (1998) 295–313.
[11] C.L. Wilson, K.J. Heppner, P.A. Labosky, B.L.M. Hogan, L.M. Matrisian, Proc. Natl. Acad. Sci. USA 94 (1997) 1402–1407.
[12] L.J. Denis, L. Verweij, Invest. New Drugs 15 (1997) 175–185.

[13] M.J. Duffy, K. McCarthy, Int. J. Oncol. 12 (1998) 1343–1348.
[14] L. Poulouin, O. Gallet, M. Rouahi, J.-M. Imhoff, Protein Expr. Purif. 17 (1999) 146–152.
[15] M.W. Mosesson, R.A. Umfleet, J. Biol. Chem. 21 (1970) 5728–5736.
[16] G. Sarath, R.S. De La Motte, F.W. Wagner, in: R.J. Beynon, J.S. Bonds (Eds.), Proteolytic Enzymes: A Practical Approach, IRL Press, Oxford, 1989, pp. 25–56.
[17] A. Fersht, Enzyme Structure and Mechanism, Freeman, New York, 1985.
[18] J.E. Schwarzbauer, J.L. Sechler, Curr. Opin. Cell Biol. 11 (1999) 622–627.
[19] A. Shaub, Nat. Cell Biol. 1 (1999) E173–E175.
[20] R.I. Manabe, N. Oh-e, T. Maeda, T. Fukada, K. Sekiguchi, J. Cell Biol. 139 (1997) 295–307.
[21] R.O. Hynes, Proc. Natl. Acad. Sci. USA 96 (1999) 2588–2590.
[22] E. Ruoslahti, Adv. Cancer Res. 76 (1999) 1–20.
[23] S.A. Corbett, L. Lee, C.L. Wilson, J.E. Schwarzbauer, J. Biol. Chem. 272 (1997) 24999–25005.
[24] K. Kolev, K. Tenekedjiev, E. Komorowicz, R. Machovich, J. Biol. Chem. 272 (1997) 13666–13675.
[25] I.H. Segel, Enzyme Kinetics, Wiley Interscience, New York, 1993.
[26] M. Adam, D. Lairez, in: Cohen-Addad (Ed.), Physical Properties of Polymeric Gels, Wiley, Chichester, 1996, pp. 87–142.
[27] P.-G. de Gennes, Scaling Concepts in Polymer Physics, 4th ed., Cornell University Press, Ithaca, NY, 1993.
[28] P.J. Flory, J. Am. Chem. Soc. 63 (1941) 3083–3100.
[29] D. Stauffer, Introduction to Percolation Theory, Taylor and Francis, London, 1985.
[30] H.E. Stanley, Introduction to Phase Transitions and Critical Phenomena, Clarendon Press, Oxford, 1971.
[31] R.J. Pelham, Y.-L. Wang, Proc. Natl. Acad. Sci. USA 94 (1997) 13661–13665.
[32] D. Choquet, D.P. Felsenfeld, M. Sheetz, Cell 88 (1997) 39–48.
[33] B.-Z. Katz, E. Zamir, A. Bershadsky, Z. Kam, K.M. Yamada, B. Geiger, Mol. Biol. Cell 11 (2000) 1047–1060.
[34] A.T. Metters, C.N. Bowman, K.S. Anseth, J. Phys. Chem. B 104 (2000) 7043–7049.
[35] A.T. Metters, K.S. Anseth, C.N. Bowman, Polymer 41 (2000) 3993–4004.
[36] M. Daoud, J. Physique 40 (1979) 201–205.